THE JOURNAL OF PHYSICAL CHEMISTRY Letters

Letter

pubs.acs.org/JPCL

Vibrational State-Selective Resonant Two-Photon Photoelectron Spectroscopy of AuS^- via a Spin-Forbidden Excited State

Hong-Tao Liu,[†,‡] Dao-Ling Huang,[†] Yuan Liu,[§] Ling-Fung Cheung,[§] Phuong Diem Dau,[†] Chuan-Gang Ning,[§] and Lai-Sheng Wang*[,†]

[†]Department of Chemistry, Brown University, Providence, Rhode Island 02912, United States

[‡]Shanghai Institute of Applied Physics, Chinese Academy of Sciences, Shanghai 201800, China

[§]Department of Physics, State Key Laboratory of Low-Dimensional Quantum Physics, Tsinghua University, Beijing 100084, China

ABSTRACT: Vibrational state-selective resonant two-photon photoelectron spectra have been obtained via a triplet intermediate state ($^3\Sigma^-$) of AuS^- near its detachment threshold using high-resolution photoelectron imaging of cryogenically cooled AuS^- anions. Four vibrational levels of the $^3\Sigma^-$ excited state are observed to be below the detachment threshold. Resonant two-photon absorptions through these levels yield vibrational state-selective photoelectron spectra to the $^2\Sigma$ final state of neutral AuS with broad and drastically different Franck−Condon distributions, reflecting the symmetries of the vibrational wave functions of the $^3\Sigma^-$ intermediate state. The $^3\Sigma^-$ excited state is spin-forbidden from the $^1\Sigma^+$ ground state of AuS^- and is accessed due to strong relativistic effects. The nature of the $^3\Sigma^-$ excited state is confirmed by angular distributions of the photoelectron images and quantum calculations.

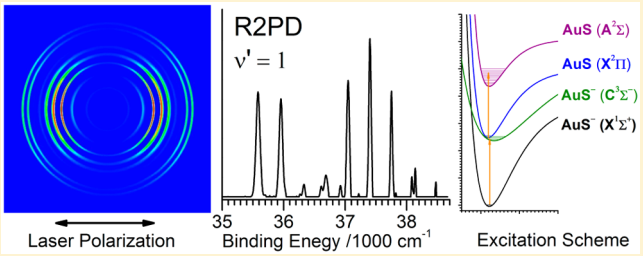

Spin is an intrinsic form of angular momentum of the electron and is responsible for many microscopic and macroscopic quantum-mechanical phenomena. The spin of a quantum system is usually conserved during electronic transitions, giving rise to the spin selection rule. This rule is strictly obeyed for electronic excitations in molecules of light elements. However, spin-forbidden transitions can happen for molecular systems containing heavy elements due to strong relativistic effects.[1] Spin-forbidden transitions are commonly observed in neutral systems and are rarely observed for a negative ion. This is primarily due to the fact that negative ions usually do not have bound *valence* electronically excited states below the electron detachment threshold. The C_2^- species was the first anion observed to have a bound *valence* electronic excited state.[2−4] Since then, a number of negatively charged ions with bound *valence* electronic excited states have been reported and used to obtain high resolution spectroscopy of anions using resonant two-photon detachment (R2PD) spectroscopy.[5−9] However, quantum state resolved photoelectron spectroscopy (PES) via excited states of anions has not been realized. R2PD−PES of the WO_2^- anion has been reported recently via a possible spin-forbidden excited state.[10] However, the R2PD−PE spectra of WO_2^- were plagued by complex vibronic structures due to large structural changes, congested electronic states, and vibrational hot bands.

Here we report the observation of a bound *valence* excited state ($^3\Sigma^-$) of AuS^-, 0.1089 eV below its detachment threshold. An excitation spectrum is obtained from the vibrationally cold AuS^- ground state ($^1\Sigma^+$) to the spin-forbidden $^3\Sigma^-$ excited state. Eight vibrational levels are observed with four below and four above the detachment threshold. Vibrational state-selective R2PD−PE spectra are obtained from the four bound vibrational levels to the $^2\Sigma$ neutral state of AuS with broad Franck−Condon distributions using high-resolution PE imaging. Spin−spin splittings are also resolved in some of the vibrational peaks in the R2PD−PE spectra.

The experiment was carried out on our electrospray PES apparatus,[11] that has been revamped with a cryogenically controlled ion trap[12,13] and a high-resolution PE imaging system.[14] Gold can form a strong covalent bond with sulfur,[15] and the Au−S bonding is known to be stronger than that of Au−O.[16] Recently, we have carried out a PES study on $[CH_3S{-}Au{-}SCH_3]^-$,[17] which is the "staple" for thiolate gold nanoparticles.[18] During this experiment, a number of fragment anions, such as Au^- and AuH_2^-,[19] were observed as a result of collision-induced dissociation (CID) of $Au(SCH_3)_2^-$ in our electrospray ionization (ESI) source. We found that the ESI conditions can be tuned to optimize the production of certain CID product, such as AuS^-. With our newly built low temperature ion trap,[12,13] the AuS^- anions were cooled to a much lower vibrational temperature (4.5 K ion trap temperature) than the previous supersonic cluster source.[16] The cooled AuS^- anions were then pulsed into the extraction zone of a time-of-flight mass spectrometer. The selected AuS^- anions were photodetached by the output of a dye laser in the interaction zone of a high-resolution velocity-map imaging

Received: January 10, 2015
Accepted: January 30, 2015
Published: January 30, 2015

DOI: 10.1021/acs.jpclett.5b00053
J. Phys. Chem. Lett. 2015, 6, 637−642

system.[14] The capabilities of our new imaging system have been demonstrated in a series of recent studies from simple molecular systems[20−22] to complex anions.[23−25] The imaging system was calibrated using the known spectra of Au^-. To search for possible resonances and excited states, we scanned the dye laser around the photodetachment threshold of AuS^- to look for either R2PD or autodetachment signals.

Figure 1 shows the photodetachment spectrum of cold AuS^- as a function of the laser photon energy by monitoring the total

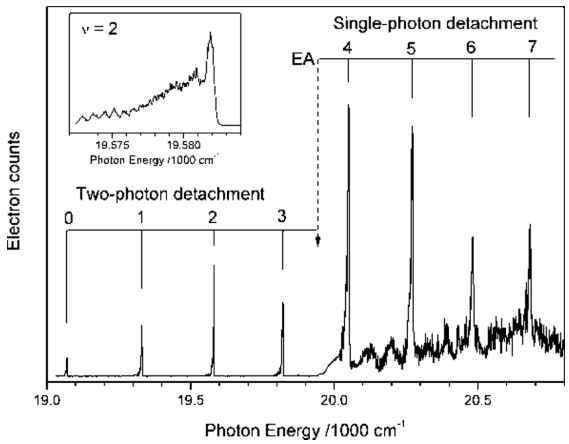

Figure 1. Single-color photodetachment spectrum of cold AuS^- via an electronic excited state around the detachment threshold. The dashed arrow indicates the electron detachment threshold of AuS^- or the electron affinity (EA) of AuS at 19 949 ± 4 cm^{-1}. The inset shows the expanded view of the rotational profile of the transition to $v' = 2$.

electron yield. Eight sharp peaks with almost equal spacing were observed, as labeled from 0 to 7. The dashed arrow indicates the detachment threshold of AuS^- or the electron affinity (EA) of AuS, which was measured accurately as 19 949 ± 4 cm^{-1} (2.4734 ± 0.0005 eV) compared with previously reported values of 2.475 ± 0.015 eV[16] or 2.469 ± 0.006 eV.[26] The spectrum recorded above the EA is the results of single-photon absorption; four resonant-enhanced autodetachment peaks (peaks 4−7) with broader line widths (fwhm ∼8 cm^{-1}) were observed. Below the threshold, there are four peaks (0−3) with zero background, which are the results of R2PD. The eight observed peaks should be due to a single vibrational progression of an electronically excited state of AuS^-. The peak with the lowest photon energy at 19 071 cm^{-1} (524.36 nm) in Figure 1 is assigned as the vibrational ground state because we did not observe any more vibrational peaks when the laser was scanned to lower photon energies. Thus, the observed excited state of AuS^- is 878 ± 4 cm^{-1} (0.1089 ± 0.0005 eV) below the detachment threshold of AuS^-. The vibrational progression can be fitted by $\omega_e - 2(v' + 1)\omega_e\chi_e$ to yield ω_e = 270 ± 4 cm^{-1} and $\omega_e\chi_e$ = 5 ± 2 cm^{-1}. The fundamental vibrational frequency for the AuS^- excited state is determined as 260 ± 4 cm^{-1}. The first four vibrational levels of the excited state are bound states and long-lived, consistent with their sharp line widths limited only by the laser line width.[21] The inset in Figure 1 shows the partially resolved rotational profile for $v' = 2$, as we showed previously that the anions could have a rotational temperature of ∼30 K in the ion trap.[27] The four levels from $v' = 4−7$ are lifetime broadened due to autodetachment: the peak widths yield a lifetime for the autodetaching vibrational states of ∼0.66 ps.

Figure 2 shows the (1 + 1) two-photon PE spectrum of AuS^- when the excitation laser wavelength was tuned to be in

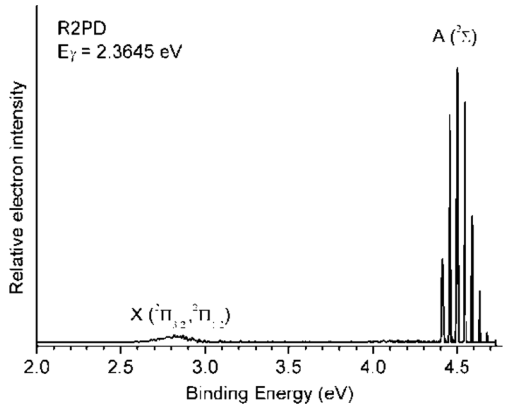

Figure 2. Resonant two-photon photoelectron spectrum of AuS^- recorded at 524.36 nm (photon energy E_γ = 2.3645 eV) via the vibrational ground state ($v' = 0$) of the intermediate excited state of AuS^-.

resonance with the transition to the $v' = 0$ level of the excited state of AuS^- at 524.36 nm (E_γ = 2.3645 eV or 19 071 cm^{-1}). Two detachment bands were observed, corresponding to the ground state ($X^2\Pi_{3/2,1/2}$) and first excited state ($A^2\Sigma$) of neutral AuS, respectively.[16] The ground state electron configuration of AuS^- ($^1\Sigma^+$) is $1\sigma^2\pi^4\delta^4 2\sigma^2\pi^{*4}$; in single-photon nonresonant PES, the $X^2\Pi$ and $A^2\Sigma$ states of AuS are accessed by electron detachment from the π^* and 2σ orbitals, respectively.[16] There are two major differences between the R2PD−PE spectrum in Figure 2 and the single-photon PE spectra: (1) the relative intensity of the X band is much weaker in the R2PD−PE spectrum and (2) the Franck−Condon envelopes of the two bands are much broader in the R2PD−PES, in comparison to the previous single-photon nonresonant PE spectra, which show almost no Franck−Condon activities for either the X or A band.[16,26] This is because of the fact that the 2σ and π^* orbitals are relatively nonbonding, as confirmed by the similar vibrational frequencies of the X and A states of AuS and that of AuS^-.[16] The spectrum in Figure 2 yielded a much more accurate vibrational frequency of 380 ± 4 cm^{-1} for the $A^2\Sigma$ state of AuS, compared to that obtained from the previous study (400 ± 60 cm^{-1}).[16] The R2PD−PE spectrum is determined by the nature of the excited state of AuS^-. The much lower vibrational frequency (260 ± 4 cm^{-1}) of the excited state of AuS^- suggests that this state corresponds to a much weaker Au−S bond with a longer Au−S bond length, resulting in the broad Franck−Condon envelopes due to the transition from this excited state to the final neutral $X^2\Pi$ and $A^2\Sigma$ states with shorter Au−S bond lengths.

We tuned the detachment laser to be in resonance with $v' = 1−3$ of the AuS^- excited state and obtained a set of vibrational state-selective R2PD−PE spectra, as shown in Figure 3, where only transitions to the $A^2\Sigma$ final state of neutral AuS are shown, along with PE images reconstructed using the pBASEX method.[28] Because of the lower spectral resolution in the energy region of the $X^2\Pi$ band, no fine features were resolved and they are not shown in Figure 3. The R2PD photoelectron angular distributions exhibit *p*-wave characters, suggesting that an *s*-type or σ electron is detached from the excited state of AuS^- to the $A^2\Sigma$ final state.[29] The series of peaks correspond to the different vibrational states of the AuS $^2\Sigma$ final state. The

DOI: 10.1021/acs.jpclett.5b00053
J. Phys. Chem. Lett. 2015, 6, 637−642

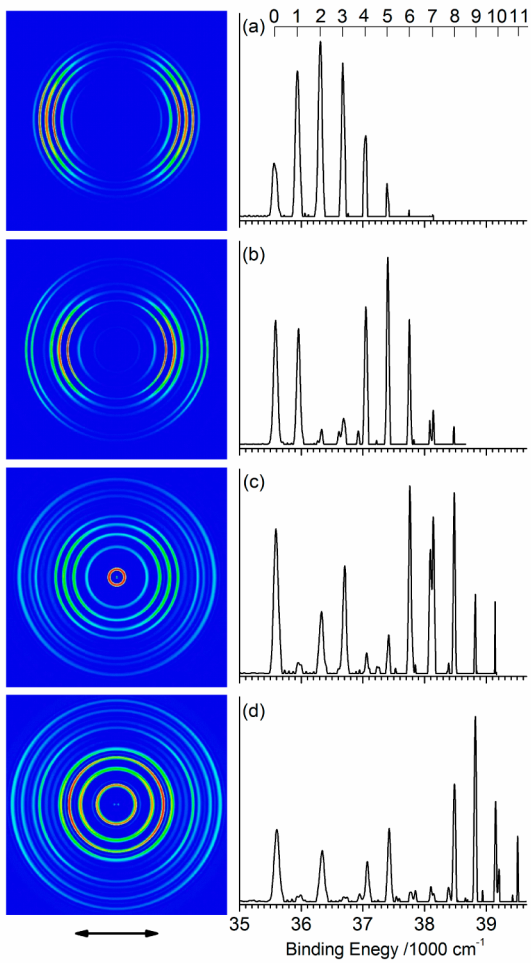

Figure 3. Resonant two-photon photoelectron images and spectra through the vibrational levels (v') of the excited state of AuS^-. Only the A band in each case is shown (see Figure 2). (a) $v' = 0$, $E_\gamma = 2.3645$ eV (same as in Figure 2); (b) $v' = 1$, $E_\gamma = 2.3968$ eV; (c) $v' = 2$, $E_\gamma = 2.4279$ eV; (d) $v' = 3$, $E_\gamma = 2.4576$ eV. The double arrow indicates the laser polarization. The vibrational quantum number v'' of the final AuS ($A^2\Sigma$) state is marked on the top.

vibrational quantum number v'' is marked on the top of Figure 3. The drastically different Franck–Condon envelopes reflect the symmetries of the vibrational wave functions of the intermediate state of AuS^-. Such vibrational state-selective PE spectra have not been seen before for anions, even though they have been observed for neutral molecules via valence excited states or Rydberg states in resonant multiphoton ionization PES.[30−37]

However, when we tuned the detachment laser to be in resonance with the $v' = 4–7$ vibrational levels, only single-photon nonresonant detachment or autodetachment to the ground state of AuS was observed (Figure 4). No R2PD signals were observed because of the short lifetime of these autodetaching vibrational states (~0.66 ps), relative to our nanosecond laser pulses.

Upon careful examination, we find that some vibrational peaks exhibit a splitting, as seen in Figure 3b–d. For example, the $v'' = 7$ peak has a splitting of about 50 cm^{-1}, which could be due to spin–orbit or spin–spin coupling in the intermediate state of AuS^-. We further performed Franck–Condon simulations by assuming Morse potentials for both the anion excited state and the neutral $^2\Sigma$ state using the PESCAL

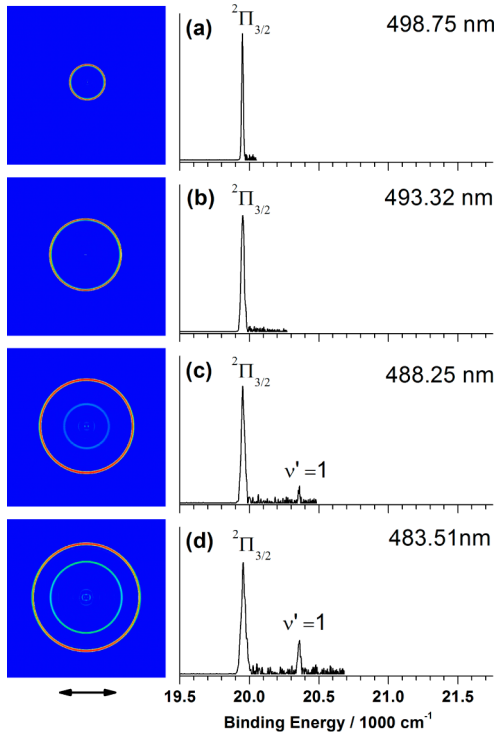

Figure 4. Resonance-enhanced photoelectron images and spectra of AuS^- through the vibrational levels (v') of the C $^3\Sigma^-$ excited state above the detachment threshold of AuS^-. (a) $v' = 4$, $E_\gamma = 2.4859$ eV; (b) $v' = 5$, $E_\gamma = 2.5133$ eV; (c) $v' = 6$, $E_\gamma = 2.5393$ eV; (d) $v' = 7$, $E_\gamma = 2.5642$ eV. The double arrow indicates the laser polarization. The electron signals were due to a combination of autodetachment and single-photon nonresonant photodetachment.

program,[38] as shown in Figure 5. We found excellent agreement between the simulated spectrum and the R2PD–PE spectrum from the $v' = 0$ level. But the agreement deteriorates for the R2PD–PE spectra from the $v' = 1–3$ levels, suggesting that the Morse oscillator is not a good approximation for the higher v' levels of the intermediate state of AuS^-, as can already be seen by the large anharmonicity. In the simulation, we used $R_e = 2.20$ Å for the $A^2\Sigma$ state of AuS and obtained a R_e of 2.33 Å for the intermediate state of AuS^-. The R_e value for the $A^2\Sigma$ state was not known. It was taken to be similar to that of the anion ground state on the basis of the observed photoelectron spectrum.[16] Thus, the obtained R_e value for the intermediate state of AuS^- should be viewed as a rough estimate.

The ground state of AuS^- has a closed-shell electron configuration, $1\sigma^2\pi^4\delta^4 2\sigma^2\pi^{*4}$ ($X^1\Sigma^+$), and an antibonding σ^* lowest unoccupied molecular orbital (LUMO).[16,26] The π^* highest occupied molecular orbital (HOMO) and the 2σ HOMO-1 are relatively nonbonding, as shown from the previous PES studies.[16,26] The observed intermediate state of AuS^- could be due to excitation of either a nonbonding HOMO or HOMO-1 electron to the antibonding LUMO, resulting in a weaker Au–S bond and a longer bond length. In order to identify the observed AuS^- excited state, we performed high-level multireference configuration interaction (MR-CI) calculations for all possible excited states from these electronic excitations. The spin–orbit coupling MR-CI method was used. The energy-consistent ECP60MDF_AV5Z basis sets for Au, aug-cc-pV5Z full-electron basis sets for S atom were used. The active space, consisting of $(9–11)\sigma$ and $(4–5)\pi$ molecular orbitals of AuS^-, was used for both the MCSCF and the MRCI

DOI: 10.1021/acs.jpclett.5b00053
J. Phys. Chem. Lett. 2015, 6, 637–642

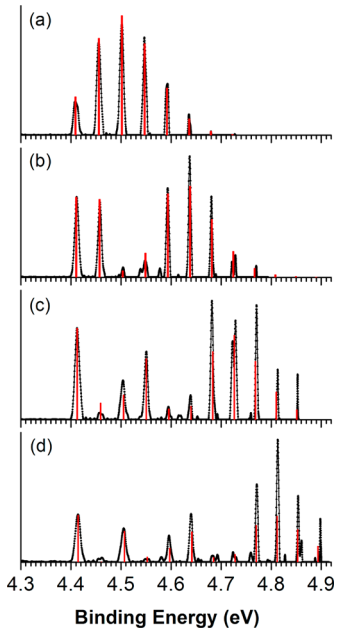

Figure 5. Franck−Condon simulation by assuming Morse potentials for both the $^3\Sigma^-$ intermediate state of AuS^- and the $^2\Sigma$ neutral final state of AuS in comparison with the experimental spectra. The heights of the red vertical bars are the calculated Franck−Condon factors. The dots are measured photoelectron spectra. (a) $v' = 0$, $E_\gamma = 2.3645$ eV; (b) $v' = 1$, $E_\gamma = 2.3968$ eV; (c) $v' = 2$, $E_\gamma = 2.4279$ eV; (d) $v' = 3$, $E_\gamma = 2.4576$ eV.

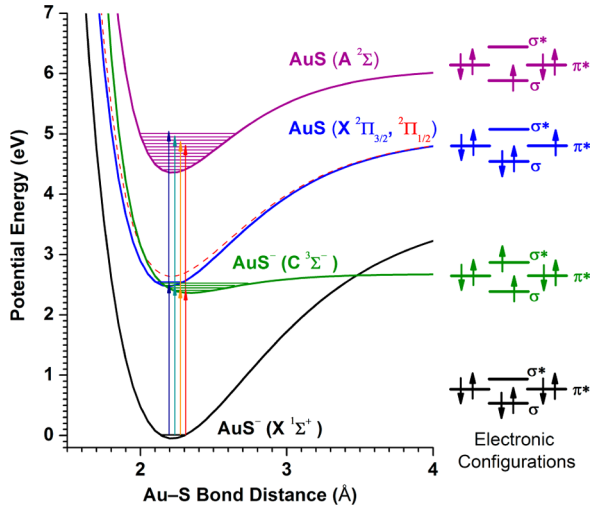

Figure 6. Schematic potential energy curves of the AuS^- (X $^1\Sigma^+$), AuS^- (C $^3\Sigma^-$), AuS (X $^2\Pi_{3/2}$, $^2\Pi_{1/2}$), and AuS (A $^2\Sigma$) states. The arrows indicate the excitations to the four bound vibrational levels of the intermediate state (C $^3\Sigma^-$) of AuS^-, corresponding to $v' = 0$−3 in Figures 1 and 3. The related electronic configurations are shown in the right. All the energies and vibrational levels are from the current work, whereas the equilibrium bond lengths for the ground state of AuS^- and AuS are from ref 16.

calculations. The bond length was varied from 1.8 to 6 Å. All calculations were carried out using the Molpro package. The basis sets ECP60MDF_AV5Z for Au and aug-cc-pV5Z for S were obtained from https://bse.pnl.gov.

Our calculations predicted two low-lying excited Π states for AuS^- at 1.1 eV ($^3\Pi$) and 1.4 eV ($^1\Pi$) above the ground state, as a result of the HOMO → LUMO excitation ($1\sigma^2\pi^4\delta^4 2\sigma^2\pi^{*3}\sigma^{*1}$). These excited states are too low to be responsible for the observed state at 2.3645 eV. We found two Σ excited states at 2.2 eV ($^3\Sigma^-$) and 3.6 eV ($^1\Sigma^+$) above the ground state, as a result of HOMO-1 → LUMO excitation ($1\sigma^2\pi^4\delta^4 2\sigma^1\pi^{*4}\sigma^{*1}$). The $^1\Sigma^+$ state seems to be too high to be responsible for the observed excited state, whereas the calculated excitation energy of the $^3\Sigma^-$ state is in good agreement with the experimental observation. Although the transition from the singlet ground state of AuS^- ($^1\Sigma^+$) to the $^3\Sigma^-$ triplet state is spin-forbidden, it is likely allowed for AuS^- due to the strong relativistic effects of Au. Our calculation predicts a fairly large cross section for the $^1\Sigma^+ \rightarrow {}^3\Sigma^-$ transition for the AuS^- anion.

The $^3\Sigma^-$ excited state can explain all our experimental observations, as shown Figure 6, which displays the schematic potential energy curves of the relevant electronic states of AuS^- ($X^1\Sigma^+$, $C^3\Sigma^-$) and AuS ($X^2\Pi_{3/2,1/2}$, $A^2\Sigma$). The electron configurations of the related states are also given in Figure 6. It is seen clearly that the detachment of the σ* electron by the second photon directly leads to the $A^2\Sigma$ final state of AuS, resulting in the vibrational state-selective PE spectra shown in Figures 2 and 3 with the broad Franck−Condon envelopes. The angular distributions (Figure 3) are consistent with the detachment of the σ* electron. However, the detachment transition from the $C^3\Sigma^-$ excited state of AuS^- to the ground state of AuS is a two-electron process, which explains its low intensity as shown in Figure 2. The observed splittings in some of the vibrational peaks in Figure 3 are likely due to spin−spin couplings of the two unpaired electrons in the $C^3\Sigma^-$ intermediate state. Our calculations predict a 45 cm^{-1} splitting between the $m_s = \pm 1$ and $m_s = 0$ spin states of the $C^3\Sigma^-$ state, consistent with our observed splitting. Spin−orbit couplings are commonly observed in PES, but spin−spin couplings are usually too small to be resolved. The evidence of spin−spin splittings in the R2PD−PES spectra of AuS^- is interesting and would warrant further theoretical investigations. Finally, we should point out that low-lying excited states in anions are rare. Our theoretical predictions of the two low-lying Π excited states at 1.1 and 1.4 eV in AuS^- are also significant. It would be interesting to study them using two-color (1 + 1′) R2PD in the future.

In conclusion, we have obtained vibrational state-selective resonant two-photon photoelectron spectra for cryogenically cooled AuS^- using high-resolution photoelectron imaging. The intermediate state was found to be a spin-forbidden triplet excited state ($^3\Sigma^-$) with respect to the singlet ground state of AuS^- ($^1\Sigma^+$), but was observed due to strong relativistic effects. The triplet $^3\Sigma^-$ excited state is found to be 2.3645 ± 0.0005 eV above the ground state of AuS^-, and 0.1089 ± 0.0005 eV below the detachment threshold of 2.4734 ± 0.0005 eV. Four vibrational levels of the $^3\Sigma^-$ state are below the detachment threshold and yielded four vibrational state-selective R2PD−PE spectra with drastically different Franck−Condon profiles due to the different symmetries of the vibrational wave functions. Fine features in the R2PD−PE spectra were observed and attributed to spin−spin couplings in the $^3\Sigma^-$ intermediate state. It is shown that high-resolution photoelectron imaging combined with the cold ion-trap technology is a powerful approach to probe the vibronic fine structures and dynamics of anionic excited states. The complete elimination of vibrational hot bands will greatly simplify the spectroscopy even for complicated anionic systems.

DOI: 10.1021/acs.jpclett.5b00053
J. Phys. Chem. Lett. 2015, 6, 637−642

AUTHOR INFORMATION

Corresponding Author

* Email: Lai-Sheng_Wang@brown.edu.

Notes

The authors declare no competing financial interest.

ACKNOWLEDGMENTS

This work was supported by the National Science Foundation (CHE-1263745 to L.S.W.). C.G.N. would like to acknowledge support of the National Natural Science Foundation of China (91336104).

REFERENCES

(1) Pyykko, P. Relativistic Effects in Structural Chemistry. *Chem. Rev.* **1988**, *88*, 563−594.

(2) Lineberger, W. C.; Patterson, T. A. Two Photon Photodetachment Spectroscopy: The $C_2^{-2}\Sigma$ States. *Chem. Phys. Lett.* **1972**, *13*, 40−44.

(3) Jones, P. L.; Mead, R. D.; Kohler, B. E.; Rosner, S. D.; Lineberger, W. C. Photodetachment Spectroscopy of C_2^- Autodetaching Resonances. *J. Chem. Phys.* **1980**, *73*, 4419−4432.

(4) Mead, R. D.; Hefter, U.; Schulz, P. A.; Lineberger, W. C. Ultra High Resolution Spectroscopy of C_2^-: The A $^2\Pi_u$ State Characterized by Perturbation Methods. *J. Chem. Phys.* **1985**, *82*, 1723−1731.

(5) Murray, K. K.; Lykke, K. R.; Lineberger, W. C. Spectroscopy and Autodetachment Dynamics of PtN^-. *Phys. Rev. A* **1987**, *36*, 699−704.

(6) Andersen, T.; Lykke, K. R.; Neumark, D. M.; Lineberger, W. C. Autodetachment Study of the Electronic Spectroscopy of FeO^-. *J. Chem. Phys.* **1987**, *86*, 1858−1867.

(7) Brinkman, E. A.; Günther, E.; Schafer, O.; Brauman, J. I. Bound Excited Electronic States of Anions. *J. Chem. Phys.* **1994**, *100*, 1840−1848.

(8) Zhao, Y. X.; de Beer, E.; Neumark, D. M. Rotationally Resolved Spectrum of the C $^2\Pi_u \leftarrow$ X $^2\Pi_g$ Electronic Transition of C_4^- via Resonant Two-Photon Detachment Spectroscopy. *J. Chem. Phys.* **1996**, *105*, 2575−2582.

(9) Zhao, Y. X.; de Beer, E.; Xu, C. S.; Taylor, T.; Neumark, D. M. Spectroscopy and Electron Detachment Dynamics of C_4^-, C_6^-, and C_8^-. *J. Chem. Phys.* **1996**, *105*, 4905−4919.

(10) Mann, J. E.; Waller, S. E.; Rothgeb, D. W.; Jarrold, C. C. Resonant Two-Photon Detachment of WO_2^-. *Chem. Phys. Lett.* **2011**, *506*, 31−36.

(11) Wang, L. S.; Ding, C. F.; Wang, X. B.; Barlow, S. E. Photodetachment Photoelectron Spectroscopy of Multiply Charged Anions Using Electrospray Ionization. *Rev. Sci. Instrum.* **1999**, *70*, 1957−1966.

(12) Wang, X. B.; Wang, L. S. Development of a Low-Temperature Photoelectron Spectroscopy Instrument Using an Electrospray Ion Source and a Cryogenically Controlled Ion Trap. *Rev. Sci. Instrum.* **2008**, *79*, 073108.

(13) Dau, P. D.; Liu, H. T.; Huang, D. L.; Wang, L. S. Photoelectron Spectroscopy of Cold UF_5^-. *J. Chem. Phys.* **2012**, *137*, 116101.

(14) Leon, I.; Yang, Z.; Liu, H. T.; Wang, L. S. The Design and Construction of a High-Resolution Velocity-Map Imaging Apparatus for Photoelectron Spectroscopy Studies of Size-Selected Clusters. *Rev. Sci. Instrum.* **2014**, *85*, 083196.

(15) Wang, L. S. Covalent Gold. *Phys. Chem. Chem. Phys.* **2010**, *12*, 8694−8705.

(16) Zhai, H. J.; Bürgel, C.; Bonacic-Koutecky, V.; Wang, L. S. Probing the Electronic Structure and Chemical Bonding of Gold Oxides and Sulfides in AuO_n^- and AuS_n^- (n = 1, 2). *J. Am. Chem. Soc.* **2008**, *130*, 9156−9167.

(17) Ning, C. G.; Xiong, X. G.; Wang, Y. L.; Li, J.; Wang, L. S. Probing the Electronic Structure and Chemical Bonding of the "Staple" Motifs of Thiolate Gold Nanoparticles: $Au(SCH_3)_2^-$ and $Au_2(SCH_3)_3^-$. *Phys. Chem. Chem. Phys.* **2012**, *14*, 9323−9329.

(18) Jadzinsky, P. D.; Calero, G.; Ackerson, C. J.; Bushnell, D. A.; Kornberg, R. D. Structure of a Thiol Monolayer-Protected Gold Nanoparticle at 1.1 Å Resolution. *Science* **2007**, *318*, 430−433.

(19) Liu, H. T.; Wang, Y. L.; Xiong, X. G.; Dau, P. D.; Piazza, Z. A.; Huang, D. L.; Xu, C. Q.; Li, J.; Wang, L. S. The Electronic Structure and Chemical Bonding in Gold Dihydride: AuH_2^- and AuH_2. *Chem. Sci.* **2012**, *3*, 3286−3295.

(20) Leon, I.; Yang, Z.; Wang, L. S. High Resolution Photoelectron Imaging of Au_2^-. *J. Chem. Phys.* **2013**, *128*, 184304.

(21) Yang, Z.; Leon, I.; Wang, L. S. Vibrational Spectroscopy of Au_4 from High Resolution Photoelectron Imaging. *J. Chem. Phys.* **2013**, *139*, 021106.

(22) Leon, I.; Yang, Z.; Wang, L. S. Probing the Electronic Structure and Au−C Chemical Bonding in AuC_2^- and AuC_2 Using High-Resolution Photoelectron Spectroscopy. *J. Chem. Phys.* **2014**, *140*, 084303.

(23) Liu, H. T.; Ning, C. G.; Huang, D. L.; Dau, P. D.; Wang, L. S. Observation of Mode-Specific Vibrational Autodetachment from Dipole-Bound States of Cold Anions. *Angew. Chem., Int. Ed.* **2013**, *52*, 8976−8979.

(24) Lopez, G. V.; Czekner, J.; Jian, T.; Li, W. L.; Yang, Z.; Wang, L. S. Probing the Electronic and Vibrational Structure of $Au_2Al_2^-$ and Au_2Al_2 Using Photoelectron Spectroscopy and High Resolution Photoelectron Imaging. *J. Chem. Phys.* **2014**, *141*, 224309.

(25) Czekner, J.; Lopez, G. V.; Wang, L. S. High Resolution Photoelectron Imaging of UO^- and UO_2^- and the Low-Lying Electronic States and Vibrational Frequencies of UO and UO_2. *J. Chem. Phys.* **2014**, *141*, 244302.

(26) Ichino, T.; Gianola, A. J.; Andrews, D. H.; Lineberger, W. C. Photoelectron Spectroscopy of AuO^- and AuS^-. *J. Chem. Phys.* **2004**, *108*, 11307−11313.

(27) Liu, H. T.; Ning, C. G.; Huang, D. L.; Wang, L. S. Vibrational Spectroscopy of the Dehydrogenated Uracil Radical via Autodetachment of Dipole-Bound Excited States of Cold Anions. *Angew. Chem., Int. Ed.* **2014**, *53*, 2464−2468.

(28) Garcia, G. A.; Nahon, L.; Powis, I. Two-Dimensional Charged Particle Image Inversion Using a Polar Basis Function Expansion. *Rev. Sci. Instrum.* **2004**, *75*, 4989−4996.

(29) Cooper, J.; Zare, R. N. Angular Distribution of Photoelectrons. *J. Chem. Phys.* **1968**, *48*, 942−943; **1968**, *49*, 4252 (Erratum)..

(30) Hines, M. A.; Michelsen, H. A.; Zare, R. N. 2 + 1 Resonantly Enhanced Multiphoton Ionization of CO via the E $^1\Pi$−X $^1\Sigma^+$ Transition: From Measured Ion Signals to Quantitative Population Distributions. *J. Chem. Phys.* **1990**, *93*, 8557−8564.

(31) Leahy, D. J.; Reid, K. L.; Zare, R. N. Complete Description of Two-Photon (1 + 1′) Ionization of NO Deduced from Rotationally Resolved Photoelectron Angular Distributions. *J. Chem. Phys.* **1991**, *95*, 1757−1767.

(32) Kim, B.; Thantu, N.; Weber, P. M. High Resolution Photoelectron Spectroscopy: The Vibrational Spectrum of the 2-Aminopyridine Cation. *J. Chem. Phys.* **1992**, *97*, 5384−5391.

(33) Asselin, P.; Piuzzi, F.; Mons, M.; Dimicoli, I. Determination of the Vibrational Level of S_n States of Chlorobenzene by Double Resonance Multiphoton Ionization Photoelectron Spectroscopy. Evidence of IVR within These States. *Chem. Phys.* **1995**, *191*, 261−269.

(34) Glab, W. L.; Glynn, P. T.; Dehmer, P. M.; Dehmer, J. L.; Wang, K.; McKoy, B. V. Rotationally Resolved Energy-Dispersive Photoelectron Spectroscopy of H_2O: Photoionization of the C(0,0,0) State at 355 nm. *J. Chem. Phys.* **1997**, *106*, 5779−5782.

(35) Ramos, C.; Winter, P. R.; Zwier, T. S.; Pratt, S. T. Photoelectron Spectroscopy via the 1 $^1\Delta_u$ State of Diacetylene. *J. Chem. Phys.* **2002**, *116*, 4011−4022.

(36) Katayanagi, H.; Matsumoto, Y.; de Lange, C. A.; Tsubouchi, M.; Suzuki, T. One- and Two-Color Photoelectron Imaging of the CO Molecule via the B $^1\Sigma^+$ State. *J. Chem. Phys.* **2003**, *119*, 3737−3744.

(37) Hockett, P.; Staniforth, M.; Reid, K. L. Rotationally Resolved Photoelectron Angular Distributions from a Nonlinear Polyatomic Molecule. *Phys. Rev. Lett.* **2009**, *102*, 253002.

DOI: 10.1021/acs.jpclett.5b00053
J. Phys. Chem. Lett. 2015, 6, 637−642

(38) Ervin, K. M. *PASCAL*, Fortran Program, 2010.

DOI: 10.1021/acs.jpclett.5b00053
J. Phys. Chem. Lett. 2015, 6, 637−642